Control and regulation of gene expression: quantitative analysis of the expression of phosphoglycerate kinase in bloodstream form Trypanosoma brucei.

Haanstra, J.R.; Stewart, M.; Luu, V.-D.; van Tuijl, J.H.; Westerhoff, H.V.; Clayton, C.; Bakker, B.M.

published in
Journal of Biological Chemistry
2008

DOI (link to publisher)
10.1074/jbc.M705782200

document version
Publisher's PDF, also known as Version of record

THE JOURNAL OF BIOLOGICAL CHEMISTRY VOL. 283, NO. 5, pp. 2495–2507, February 1, 2008

Control and Regulation of Gene Expression

*QUANTITATIVE ANALYSIS OF THE EXPRESSION OF PHOSPHOGLYCERATE KINASE IN BLOODSTREAM FORM TRYPANOSOMA BRUCEI**[S]

Received for publication, July 13, 2007, and in revised form, October 31, 2007 Published, JBC Papers in Press, November 8, 2007, DOI 10.1074/jbc.M705782200

Jurgen R. Haanstra[‡1], Mhairi Stewart[§], Van-Duc Luu[§], Arjen van Tuijl[‡], Hans V. Westerhoff[‡¶], Christine Clayton[§2], and Barbara M. Bakker[‡2,3]

From the [‡]Vrije Universiteit, Biocentrum Amsterdam, De Boelelaan 1085, 1081 HV Amsterdam, The Netherlands, the [§]Zentrum für Molekulare Biologie der Universität Heidelberg, Im Neuenheimer Feld 282, 69120 Heidelberg, Germany, and the [¶]Manchester Centre for Integrative Systems Biology, MIB, SCEAS, the University of Manchester, Manchester M1 7ND, United Kingdom

Isoenzymes of phosphoglycerate kinase in *Trypanosoma brucei* are differentially expressed in its two main life stages. This study addresses how the organism manages to make sufficient amounts of the isoenzyme with the correct localization, which processes (transcription, splicing, and RNA degradation) control the levels of mRNAs, and how the organism regulates the switch in isoform expression. For this, we combined new quantitative measurements of phosphoglycerate kinase mRNA abundance, RNA precursor stability, *trans* splicing, and ribosome loading with published data and made a kinetic computer model. For the analysis of regulation we extended regulation analysis. Although phosphoglycerate kinase mRNAs are present at surprisingly low concentrations (*e.g.* 12 molecules per cell), its protein is highly abundant. Substantial control of mRNA and protein levels was exerted by both mRNA synthesis and degradation, whereas splicing and precursor degradation had little control on mRNA and protein concentrations. Yet regulation of mRNA levels does not occur by transcription, but by adjusting mRNA degradation. The contribution of splicing to regulation is negligible, as for all cases where splicing is faster than RNA precursor degradation.

The flux through a metabolic pathway depends on the kinetic characteristics and concentrations of the constituent enzymes, on the levels of co-enzymes, and on their compartmentation. The concentrations of the enzymes in turn depend on the rates of transcription, processing, nuclear export, translation, degradation of the mRNA, and protein processing and degradation. Because each of these levels can in principle be regulated, the challenge is how to analyze the behavior of such a complex system in terms of the underlying processes.

Metabolic control analysis (MCA)[4] and extensions that include gene expression is a powerful approach for the analysis of complex biochemical networks (1–4). In MCA, the control exerted by an enzyme on a concentration of any substance X (5) is quantified by its concentration control coefficient, which is defined as the percentage increase of the steady-state concentration of X that results from a 1% activation of the enzyme of interest. The sum of the concentration control coefficients of all the enzymes in the network is 0. This reflects that (i) activation of some enzymes increases the concentration of X, whereas activation of other enzymes should reduce the concentration of X (these enzymes have negative concentration control coefficients), and (ii) the positive controls together are equal to the negative controls. The principles of MCA do not only apply to metabolic pathways; they can also be used and extended to dissect the control distribution in regulatory pathways beyond steady state (for example see Refs.6 and 7) or gene expression cascades (for example see *e.g.* Ref. 8). Earlier MCA, as also applied to trypanosomes, has looked more at the control of fluxes, showing that usually flux control coefficients are smaller than 1, because several enzymes partially control the flux (for example see Refs. 9–11). In this study we shall focus on the control of mRNA and protein concentrations.

Questions about control (used strictly in the MCA sense) may be considered as *what if* questions. *If* the cell were to increase the concentration of a controlling enzyme or *if* a scientist were to add an inhibitor of this enzyme, the control coefficient indicates the extent to which a flux or concentration should change. Control coefficients may be viewed as the *potential* to regulate. To understand how a flux is actually regulated when the cell copes with a certain challenge, a complementary concept is required. To this aim regulation analysis has been developed. In its original form (12, 13), it dissects to what extent a metabolic flux is regulated by metabolism and to what extent by gene expression. An enzyme rate v is usually the mathematical product of the enzyme capacity V_{max}, which depends on the enzyme concentration e, and a metabolic function, which depends on metabolite concentrations M and affinity constants K as shown in Equation 1,

* This work was supported in part by a Vernieuwingsimpuls (to B. M. B.) from Netherlands Science Organization NWO, by the EC-FP6 program (through BioSim, NucSys, and EC-MOAN), the ESF program funcdyn, NWO-ALW and NWO-CLS, and by the Biotechnology and Biological Sciences Research Council (to H. V. W.). Work in the Clayton laboratory was supported by the Wellcome Trust (to M. S.) and the Deutsche Forschungsgemeinschaft. The costs of publication of this article were defrayed in part by the payment of page charges. This article must therefore be hereby marked "*advertisement*" in accordance with 18 U.S.C. Section 1734 solely to indicate this fact.

[S] The on-line version of this article (available at http://www.jbc.org) contains supplemental Table 3B, discussion of Table 5, and additional references.

[1] Recipient of a VU-FALW Rijnland fonds travel grant for a visit of six months to the Zentrum für Molekulare Biologie der Universität Heidelberg.

[2] Both authors contributed equally to this manuscript.

[3] To whom correspondence should be addressed. Tel.: 31-20-598-7196; Fax: 31-20-598-7229; E-mail: barbara.bakker@falw.vu.nl.

[4] The abbreviations used are: MCA, metabolic control analysis; UTR, untranslated region; PGK, phosphoglycerate kinase; nt, nucleotide; SL, spliced leader; EST, expressed sequence tag.

$$\nu = V_{max}(e) \times f(M,K) \quad \text{(Eq. 1)}$$

Taking the logarithm of both sides of this equation and comparing two different conditions, one obtains Equation 2,

$$\Delta \log \nu = \Delta \log V_{max}(e) + \Delta \log f(M,K) \quad \text{(Eq. 2)}$$

Dividing by $\Delta \log \nu$ yields Equation 3,

$$1 = \frac{\Delta \log V_{max}(e)}{\Delta \log \nu} + \frac{\Delta \log f(M,K)}{\Delta \log \nu} \equiv \rho_{hierarchical} + \rho_{metabolic} \quad \text{(Eq. 3)}$$

in which $\rho_{hierarchical}$ and $\rho_{metabolic}$ are the hierarchical (*i.e.* gene expression) and metabolic regulation coefficients. The hierarchy of gene expression can be further dissected to analyze regulation at the levels of transcription, precursor splicing and degradation, mRNA degradation, translation, and protein degradation (14).

In this study, we use a "bottom-up" systems biology approach (15) and the principles of MCA and regulation analysis to elucidate the control and regulation of the phosphoglycerate kinase (PGK) gene expression cascade in *Trypanosoma brucei*, a flagellated unicellular parasite. *T. brucei* multiplies as "bloodstream form" in the blood and tissue fluids of mammals and as "procyclic form" in the midgut of tsetse flies. Both forms can be maintained indefinitely in culture. In bloodstream trypanosomes, glycolysis is simple but has unique features: pyruvate is excreted as the dominant end product; nine enzymes of the glycolytic pathway and glycerol metabolism are compartmentalized in a microbody (the glycosome); and gluconeogenesis is absent. In the procyclic form, energy metabolism is more diverse, with major contributions from the mitochondrion (16).

T. brucei bloodstream form glycolysis is an attractive model to initiate quantitative studies of control and regulation, because both the glycolytic pathway and the mechanisms available for regulating gene expression are simpler than in other eukaryotes, including yeasts. The kinetic characteristics and activities of all of the (known) enzymes, and the concentrations of all the (known) metabolites, have been determined. We have previously used this information to develop a robust model of bloodstream trypanosome glycolysis, which not only explained known pathway characteristics but also predicted consequences of perturbations of the system that have since been verified experimentally (10, 11, 17–21).

Similarly, the *T. brucei* gene expression cascade is simpler than that of other organisms, because transcription by RNA polymerase II appears to be constant for all genes during exponential growth. The protein-encoding genes are organized in polycistronic transcription units that may contain 100 or more open reading frames; promoters for these have previously proven elusive (22–24). Mature mRNAs are formed through co-transcriptional 5′-*trans* splicing of a capped 39-nucleotide spliced leader (SL), and coupled 3′-polyadenylation (25). Thus, in contrast to nearly all other organisms from prokaryotes to man, trypanosome gene organization precludes the differential regulation of expression of individual protein-coding genes at the level of transcription initiation. Alternative regulation points are RNA processing, export from the nucleus, translation, and degradation. So far, there is strong evidence only for regulation of mRNA degradation and translation (26), but the strength of this regulation is unclear.

There are three *PGK* genes in the trypanosome genome, *i.e. PGKA*, *PGKB,* and *PGKC*. They are adjacent to each other in a single transcriptional unit (27). Although the three *PGK* genes are co-transcribed, they have different expression patterns (27). The PGKA protein and mRNA are present at low levels in the glycosomes of all life stages of the parasite (28, 29). PGKB and PGKC have distinct expression patterns as follows. The cytosolic PGKB protein and its mRNA are predominantly expressed in the procyclic form, and the glycosomally localized PGKC isoenzyme (and the *PGKC* mRNA) is the predominant isoenzyme in the bloodstream form (27, 30). The total cellular PGK activity does not differ much between bloodstream- and insect form trypanosomes. However, correct localization of PGK activity, and hence regulation of PGKB and PGKC expression, are vital, because cytosolic PGK activity causes growth arrest of bloodstream form trypanosomes (31). Qualitatively, the expression patterns of the isoenzymes can be explained by the different stabilities of their mature mRNAs, depending on their 3′-untranslated regions (UTRs) (32–36). There might be additional regulation at the levels of splicing (37, 38), translation (39), and variations in protein stability, but the quantitative importance of these processes is unknown, and there has not been a methodology even to establish this.

In this study we developed this methodology and applied it to the PGK isoenzyme expression in *T. brucei*. We measured accessible properties of the expression of the *PGKB* and *PGKC* genes and analyzed the distribution of control and regulation of the expression of the PGK locus. We built a quantitative computer model of the bloodstream form to help us do this. We found that in bloodstream form trypanosomes the control of the *PGK* mRNA concentrations is distributed between transcription, splicing, and mRNA degradation, whereas *T. brucei* only uses mRNA degradation to regulate the *PGK* mRNA concentrations when it differentiates from the bloodstream to the insect form.

EXPERIMENTAL PROCEDURES

Cell Culture—Bloodstream form cell line BF449 (40) was cultivated in HMI-9 medium supplemented with 10% fetal calf serum (Invitrogen) and 0.2 μg/ml phleomycin (Cayla) in an air-saturated incubator at 37 °C and 5% CO_2. Procyclic PF449 was cultivated in SDM-79 medium with 10% fetal calf serum (Invitrogen) and 0.2 μg/ml phleomycin in closed culture flasks at 30 °C (41).

RNA Isolation and Quantification of Mature TUBA and PGK mRNA—Total RNA was isolated in the exponential phase of growth (bloodstream forms maximally 2×10^6 cells/ml and procyclic cells maximally 5×10^6 cells/ml), using peqGOLD-Trifast (peqLab) or TRIzol (Invitrogen) according to the manufacturer's instructions. Tracer RNAs were made from a 983-bp fragment of the α-tubulin (*TUBA*) gene (positions 3–986) cloned into pGEMTeasy (pHD1792), and gPGK44-1, which contains the PGKC coding region plus 33 bp of its 5′-UTR (42). Northern blot analysis confirmed the presence of

a single length product. The plasmid DNAs were linearized with SpeI or XhoI, respectively, and transcribed by T7 polymerase or, alternatively, linearized with BamHI and transcribed with T3 polymerase. To measure the yield of mRNA, the tubulin tracer was added to either the Trifast solution or the purified RNA; the relative intensities of the tubulin signals were measured after Northern blotting. The average yield of this RNA was 55%.

Total RNA was denatured in formamide at 95 °C and separated by electrophoresis on formaldehyde/formamide-agarose gels. The RNA was blotted onto neutral nylon membranes (Nytran), stained with methylene blue to check for even transfer, and then hybridized with the *PGK* or *TUBA* probe tracer fragments that had been labeled by random priming or PCR with ^{32}P-labeled nucleotides. *SRP* RNA (43) was used as a loading control. Signals were detected and measured by phosphorimaging. To quantify the absolute amounts of *PGK* or *TUBA* mRNA in trypanosomes, various known amounts of the pure tracer mRNAs (see above) were added to the lysate before mRNA isolation. To calculate the amounts back into molecule numbers, we used mature and precursor RNA lengths and assumed a mean nucleotide monophosphate mass of 339 g/mol.

Ribonuclease Protection Assay—To quantify kinetics of precursor splicing and degradation, exponentially growing cell cultures with a density of $1–2 \times 10^6$ cells/ml were incubated either with Sinefungin (1 or 2 μg/ml) for 30 min with subsequent incubation with actinomycin D (10 μg/ml) for 0–25 min or with actinomycin D alone. Cells were pelleted by centrifugation, after which supernatant was removed and pellet was taken up in TRIzol (Invitrogen) for total RNA isolation. The RNase protection probe for measurement of PGKB/C processing was a BamHI-SpeI fragment subcloned from pHD1417 (34) into pBluescript KS (pHD1402). The fragment contains the regions from the PGKB stop codon to the PGKC start codon, without the regulatory U-rich element. As a control for product identification, a similar construct with the U-rich element present was also used (pHD1402). RNase protection assays with the full-length probe yielded multiple products, presumably because of "breathing" of A-U rich hybrids. The full-length probe therefore could not be used for quantification of precursor. The plasmids were cut with SalI, and probes were transcribed by T7 polymerase (MAXIscript, Ambion) in the presence of ATP, CTP, GTP, and [α-^{32}P]UTP. RNase protection analysis was performed using RNase protection analysis III kit (Ambion). Each RNase protection reaction included 10 μg of trypanosome RNA and 8×10^4 cpm of probe (Cerenkov counts). If twice as much probe was used, the signals were similar indicating that probe was in excess. A ^{32}P-labeled 10-bp Invitrogen DNA ladder served as a size marker. Products were run on 5% denaturing polyacrylamide/urea gels for 4–6 h, removed from the glass plates, put onto a piece of Whatman paper, and vacuum-dried overnight. Controls contained only 1×10^4 cpm of probe. Signals were detected and measured by phosphorimaging. Degradation curves were analyzed using the Kaleidagraph program. To check the precursor status of band "a," we used RNA prepared from trypanosome with inducible RNA interference against SMD1 (44) or cleavage and polyadenylation factor CPSF30 (45). The identities of bands were confirmed by using shorter probes specific for the 5′ end of the PGKC mRNA and the spacer region, and by assessing stage specificity (not shown).

Polysome Analysis—Polysomes were isolated as described in Ref. 46. RNA was purified as described above, and the distribution of different RNAs was analyzed by Northern blotting.

Purification of TbPGKC—*Escherichia coli* BL21(DE3)pLysS cells (a kind gift of Prof. P. Michels) containing the plasmid TbPGKC (47) were grown, treated with isopropyl 1-thio-β-D-galactopyranoside to induce TbPGKC expression, and harvested according to the published protocol. In short, cells were harvested and lysed, and nucleic acids were digested, and lysates were treated with protamine sulfate. The supernatant was then concentrated with a YM-10 filter and applied to a Resource S column (Amersham Biosciences) connected to an Akta Explorer fast protein liquid chromatography (Amersham Biosciences). Proteins were eluted with a linear gradient of 50–400 mM NaCl in the loading buffer. Peak fractions from column purification were tested enzymatically for PGK activity, and the samples with activity were evaluated on a silver-stained SDS-polyacrylamide gel. All fractions that had PGK activity were >90% pure (as judged from Coomassie Blue and Silver staining of SDS-polyacrylamide gels; data not shown). This was pure enough to enable us to use the fractions as standards on Western blots. Protein concentration was determined with a BCA (Pierce) assay using bovine serum albumin (Pierce) as a standard.

Quantitative Immunoblotting—For each sample 3×10^6 cells were harvested by centrifugation, washed in phosphate-buffered saline, and finally resuspended in 15 μl of phosphate-buffered saline and 15 μl of Laemmli buffer. Samples were stored at −80 °C before analysis.

Protein samples and purified TbPGKC were boiled for 5–10 min at 95 °C and run on an SDS-polyacrylamide gel (12%). As gel and transfer inhomogeneities are the major source of correlated errors in immunoblotting (48), we randomized samples on every blot. Proteins were transferred to a methanol-activated polyvinylidene difluoride membrane (Bio-Rad) by blotting overnight at 4 °C and 20V. Membranes were subsequently placed for 1 h in block buffer, containing 5% (w/v) skim milk powder in TBST (Tris-buffered saline with 0.05% (v/v) Tween 80)). After five wash steps in TBST the blot was submerged in block buffer with PGKC antibody Do425 (kind gift from Prof. Paul Michels; raised against recombinant PGKC (47)) (1:10,000) for 1 h. After washing, blots were put in block buffer with horseradish peroxidase-linked anti-rabbit IgG (DAKO A/S, Denmark) (1:2000) for 1 h and washed in TBST, and horseradish peroxidase activity was measured after a 2-min incubation with LumilightPLUS Western blotting substrate (Roche Applied Science). Quantitation was done with Quantity One software (Bio-Rad) by total surface scan, which was corrected for differences in spot width. With different dilutions of cell lysate and standard it was checked if the appearing bands were in the linear range of the blot. Background was subtracted from the PGKC bands, and for each separate blot, the PGKC band was compared with the standards so as to obtain the mass of the PGKC in the cell lysate lanes. From the number of cells in the

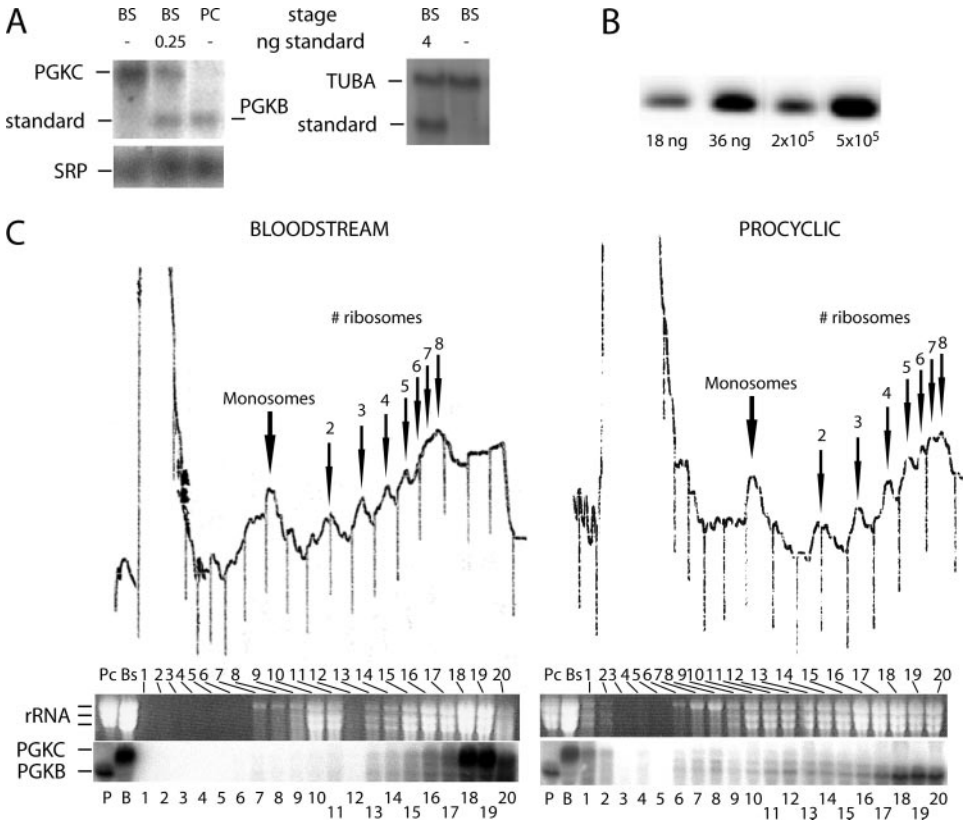

FIGURE 1. *A,* quantitation of *PGKC* and *PGKB* mRNA levels. Northern blot analysis of *PGKB* (*lower band*) and *PGKC* (*upper band*) transcripts in 4×10^7 bloodstream (*Bs*) or procyclic (*Pc*) cells. *In vitro* transcribed *PGK* mRNA (0.25 ng) was added to the BS+ lysate prior to RNA preparation. *SRP* was used as a loading control. *B,* quantitation of PGKC protein levels. Recombinant TbPGKC and bloodstream form lysates were separated by SDS-PAGE and blotted onto a polyvinylidene difluoride membrane. The band around 50 kDa is shown. The *numbers below* indicate protein amount (for standards) or the number of cells. *C,* association of *PGK* mRNA with polysomes in bloodstream trypanosomes. Sucrose gradient fractions from bloodstream form (*Bs*) (*left*) or procyclic (*Pc*) (*right*) trypanosomes were analyzed by spectrophotometry (A_{280}), then RNA was extracted and *PGK* mRNA detected by Northern blotting. On the *upper panel* showing the A_{280} trace, with downward fraction markers, the approximate ribosome numbers are indicated. The fraction numbers are indicated *below* the trace. RNA corresponding to the fractions is shown below. The ethidium bromide stain shows the three ribosomal RNAs, and the Northern blot was probed with a *PGK* probe. Pure bloodstream (*Bs*) and procyclic (*Pc*) total RNAs are included as controls.

lysate (determined by cell count), the molecular weight of the protein (47 kDa), and Avogadro's number, we calculated the number of PGKC molecules per cell.

Calculations and Graphs—Steady-state calculations were done in Excel (Microsoft). Data were plotted with Sigmaplot or Kaleidograph. The transcription model for PGK was constructed in Jarnac 2.0 (49, 50).

Jarnac calculates the control coefficient of any process i on any steady-state concentration X numerically by varying a parameter *pi* that linearly affects a rate v_i, by a small percentage, from Equation 4,

$$C_i^x = \left(\frac{\Delta X/X}{\Delta p_i/p_i}\right)_{\text{steady state}} \Bigg/ \left(\frac{\Delta v_i/v_i}{\Delta p_i/p_i}\right)_{\text{instantaneous}} \qquad \text{(Eq. 4)}$$

The parameters that were varied were: $v_{\text{transcription}}$, μ, k_{degrP}, k_{splicing}, k_{degrB}, k_{degrC}, and k_{transl} (see model description or Table 1 for the meaning of these parameters).

RESULTS

To construct a quantitative model of the dynamics of PGK expression, we started by collecting quantitative data about the concentrations and turnover rates of the most important molecular players.

Amount of RNA in Trypanosomes—The total amount of RNA was measured in lysates from cultured trypanosomes to which different amounts of tracer RNA were added prior or subsequent to the isolation procedure. More than 10 measurements of each form showed that bloodstream form trypanosomes contain 0.5 ± 0.1 pg (mean ± S.E.) of total RNA per cell, whereas procyclic trypanosomes had 2.2-fold more RNA per cell. A previous estimate reported 0.8 pg per procyclic trypanosome (51). Depending on the growth conditions, *Saccharomyces cerevisiae* has 0.5–1.6 pg of RNA/cell, of which 85% is rRNA and 10% is tRNA and other small RNAs (52).

If 85% of the trypanosome RNA is ribosomal, 0.5 pg of RNA should correspond to 1.2×10^5 ribosomes. Results from purification with oligo(dT) or poly(U) affinity resins or from Northern blots suggested that trypanosome mRNA represents 5% of the total RNA or 0.025 pg/cell (53–55). Assuming an average mRNA size of 2.2 kb (see Supplemental Material), there are ~20,000 mRNA molecules per bloodstream trypanosome and 6 ribosomes per mRNA molecule.

Amounts and Turnover of PGK and TUBA mRNAs—Northern blotting with PGK standards (Fig. 1*A*) showed that bloodstream form trypanosomes contained 12.1 ± 7.7 (S.D., $n = 5$) molecules of PGKC mRNA (this study) and 15 times less PGKB mRNA per cell (33). In procyclic trypanosomes, there were 18 ± 2 (S.D., $n = 5$) PGKB mRNAs per cell, and PGKC mRNA was not detectable, as expected from previous reports (Gibson *et al.* (27); Colasante *et al.* (33)).With quantitative PCR we do detect PGKC mRNA in procyclics, but at 12 times less abundant than in bloodstream forms when compared with the housekeeping gene hypoxanthine-guanine phosphoribosyltransferase. Hypoxanthine-guanine phosphoribosyltransferase mRNA levels are similar in bloodstream and insect stages of *T. brucei* (56). For comparison we also measured the number of α-tubulin (*TUBA*) transcripts, using *TUBA* standards (Fig. 1*A*). Bloodstream form trypanosomes contained 72 ± 12 molecules of *TUBA* mRNA per cell.

Half-lives of mRNAs were measured previously. To measure mRNA decay kinetics in trypanosomes, it is necessary to inhibit mRNA processing and transcription. Using actinomycin D and Sinefungin, the half-life of *PGKC* mRNA in bloodstream trypanosomes was 45 min (33). In procyclic trypanosomes, a

reporter (chloramphenicol acetyltransferase) mRNA bearing a *PGKC* 3′-untranslated region (UTR), produced by T7 RNA polymerase, had a half-life of about 5 min (33); the low abundance of the endogenous *PGKC* mRNA in this *T. brucei* form renders direct measurement of its half-life problematic. For *PGKB*, measurements have been made using actinomycin D inhibition alone, which can result in overestimates of stability (33). A chloramphenicol acetyltransferase reporter with a *PGKB* 3′-UTR (produced by T7 polymerase) had an average half-life of about 7.5 min in bloodstream form trypanosomes (34), and the *PGKB* mRNA showed negligible decay in procyclic trypanosomes over 90 min; here we assumed a half-life of 120 min and when using this estimate we discuss its implications for our analysis of regulation (see below).

Steady-state PGK Protein Levels and Stability—We next measured the PGK protein level in bloodstream form trypanosomes. As a standard we used TbPGKC (47) (Fig. 1*B*). Comparing the PGKC amount in bloodstream form lysates to known amounts of standard on three separate Western blots in five independent samples and using a molecular mass of 47 kDa, we found $1 \times 10^6 \pm 0.5$ molecules per cell ($n = 3$; S.E., including errors between lanes of standard). PGKB could only be seen in bloodstream forms after grossly overloading the gel.

To check the stability of PGKC, we pulse-labeled bloodstream form trypanosomes for 30 min with [^{35}S]methionine and then diluted them into normal medium. PGK was immunoprecipitated; the immunoprecipitates were separated by gel electrophoresis and the proteins detected by autoradiography. As was seen previously for aldolase in procyclic forms (57), no degradation of PGKC was detected over the 8-h chase period (not shown).

Ribosome Density on PGK mRNA—To find out how many ribosomes transcribed *PGK* mRNAs simultaneously, we analyzed their distribution after sucrose gradient centrifugation. The *upper panels* of Fig. 1*C* show the overall protein levels as judged by the absorbance at 280 nm, and the *lower panels* show the ethidium bromide-stained ribosomal RNA and hybridization of a Northern blot with a *PGK* probe. In both procyclic and bloodstream trypanosomes, the *PGK* hybridization was concentrated at the bottom of the gradient. We extrapolated (using a logarithmic function) from the portion of the gradient in which individual ribosomes were visible and concluded that there were 11–14 ribosomes per *PGKC* mRNA molecule in bloodstream forms. Estimates for *PGKB* in procyclics are less accurate, but the results are consistent with a comparable ribosome density. *PGKC* mRNA was undetectable in procyclic forms. In bloodstream forms, *PGKB* mRNA appeared to be polysomal, but the interpretation was complicated by artifacts because of co-migration of the rRNA at the same position in the blot.

The Kinetics of Splicing and Precursor Degradation—To estimate the rate at which the PGK precursor RNA is *trans* spliced in bloodstream form trypanosomes, we measured the rate at which the PGK polycistronic precursor disappeared under two conditions. In one condition we inhibited transcription. In the second condition we inhibited both transcription and splicing. An RNase protection assay with an antisense probe spanning the region between the PGKC start codon and the PGKB stop codon, but excluding the U-rich regulatory region (Fig. 2*A*), resulted in bands indicated as *a*, *b*, and *c* in Fig. 2*B*. The cluster of prominent bands around 80 nucleotides corresponded to the 5′-untranslated region of the PGKC mRNA and was undetectable if procyclic RNA was used (not shown), consistent with the low abundance of PGKC mRNA in procyclics (Fig. 2, *A* and B, labeled as *c*). Just above these bands was a faint band migrating around 85 nucleotides, which was the only species observed if procyclic mRNA was used. This corresponded to the 3′-UTR of the mature PGKB mRNA (without the U-rich element) (Fig. 2, *A* and *B*, labeled as *b*). Above these bands was a product that spanned from the PGKC initiation codon to the end of the U-rich element, which is approximately the position of the PGKB polyadenylation site (Fig. 2, *A* and *B*, labeled as *a*). We took this band to correspond to the PGKB-PGKC precursor. It was more prominent in trypanosomes in which splicing was inhibited by addition of Sinefungin (Fig. 2*B*, *lanes 1* and *2*). In our calculations we assumed that it all represents precursor RNA, although some contribution from aberrantly processed mRNAs cannot be ruled out.

Actinomycin D inhibits all transcription of DNA, including that into mRNAs and spliced leader RNA (58). After addition of actinomycin D, the precursor band disappeared with a half-life of 1.4 min ($k_{\text{splicing+degradation}}$ of 0.50 min^{-1}; Fig. 2*C* and Table 1); greater precision was precluded by the mechanics of the assay, which requires diffusion of actinomycin D into the cells and a centrifugation step. To correct for degradation of precursor RNA, the cells were pretreated with Sinefungin, an inhibitor of splicing in trypanosomes (59, 60). When actinomycin D was added to these cells, the precursor decayed with a half-life of 8.2 min ($k_{\text{precursor degradation}}$ of 0.085 min^{-1}; Fig. 2, *B* and *C*, and Table 1). Assuming that the Sinefungin incubation had not affected the precursor degradation rate constant, we estimated k_{splicing} at 0.41 min^{-1}. This result indicated that in the absence of Sinefungin, ~80% of precursor disappearance was because of splicing. Preliminary measurements of *PGKC* splicing by real time PCR have been consistent with these RNase protection assays, but attempts to measure *PGKC* polyadenylation kinetics have been frustrated by the appearance of what seemed to be stable RNA species spanning the downstream intergenic region.[5]

Quantitative Computer Model of PGK Expression—Based on the data collected above and some additional information from the literature, a kinetic model of PGK expression in bloodstream form trypanosomes was constructed. Transcription rate was taken to be constant. Precursor degradation, splicing, degradation of the mature mRNAs, translation, and protein degradation were all described by linear kinetics (Fig. 3). Such linear kinetics should be obtained if the substrate or activator concentration is below the effective Michaelis-Menten or binding constant. This occurs when substrate or activator is a minority among all substrates or factors competing for the same site on the enzyme complex catalyzing the process considered. This is the situation that should be expected in this case, as the PGK RNAs and proteins are just one of many substrates for enzymes

[5] M. Stewart, unpublished results.

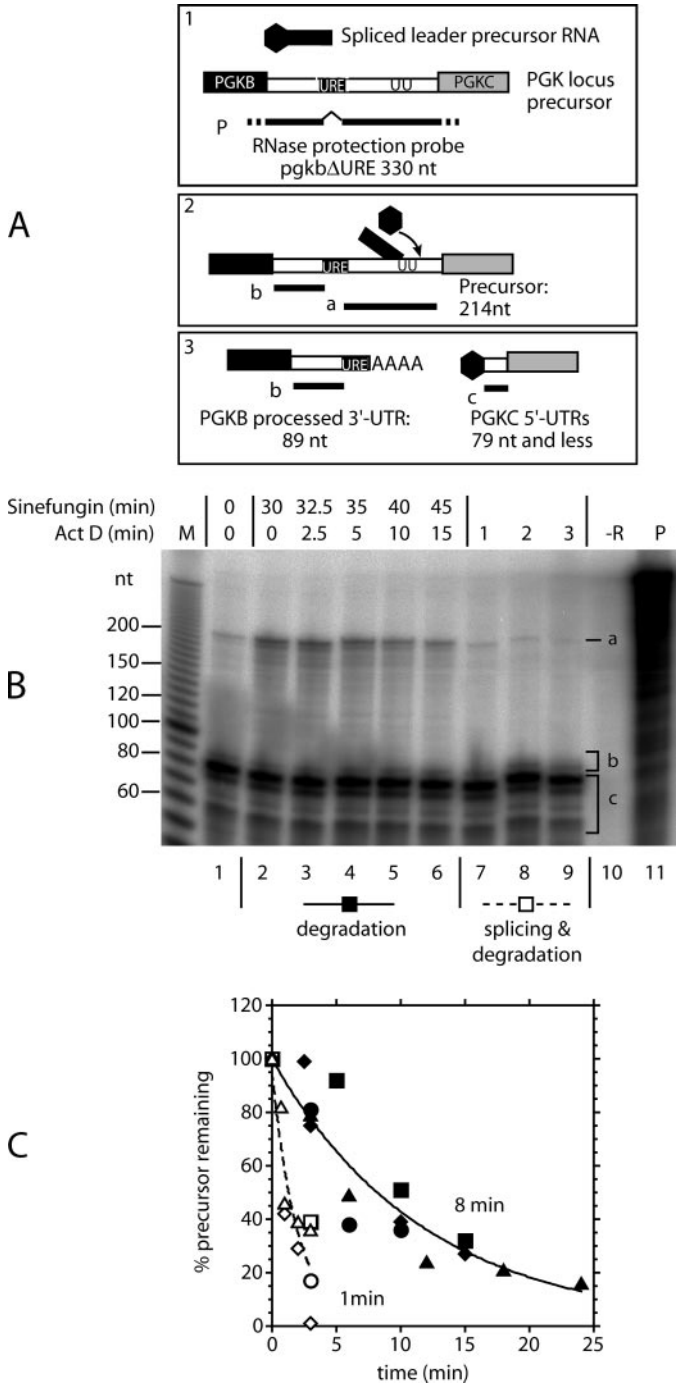

FIGURE 2. **RNase protection assays for measurement of *PGK* RNA processing.** *A, panel 1*, before processing, the primary transcript extends between the *PGKB* and *PGKC* open reading frames. The precursor and *PGKB* 3′-UTR contain a U-rich instability element (*URE, shaded*), and the precursor also has a U-rich polypyrimidine tract that signals *trans* splicing (*UU*). The 135–140-nt spliced leader precursor RNA (*black*) carries the 39-nt spliced leader (*hexagon*). The 330-nt RNase protection probe includes all of the regions between the open reading frames, apart from the instability element, and also extends at both ends through polylinker sequence. *Panel 2*, after RNase digestion, any probe that was hybridized with the precursor would be cut into 2 pieces; fragment *b* corresponds to the 3′-UTR of *PGKB*, whereas fragment *a* is diagnostic of the unspliced *PGKC* precursor. During splicing, a branch is formed upstream of the polypyrimidine tract (3). RNase protection product *b* is diagnostic of both precursor RNA and mature *PGKB*. Fragment *c* corresponds to *trans* spliced *PGKC* RNA. *B*, typical RNase protection result. Trypanosomes were incubated either with Sinefungin (1 or 2 μg/ml) plus actinomycin D (*ActD*, 10 μg/ml), indicated with *degradation* in *lanes 2–6*, or with actinomycin D alone, indicated with *splicing and degradation* in *lanes 7–9*. The time of incubation in minutes is shown *above* the lanes. *M*, marker; *−R*, no trypanosome RNA added; *P*, probe alone. *C*, quantitation of "band a" (diagnostic for precursor) in four independent experiments done on different batches of cells. Each experiment is represented by a different symbol, with *solid symbols/solid line* for precursor degradation (actinomycin D + Sinefungin), and *open symbols/dashed line* for splicing plus degradation (actinomycin D alone). The curves were fit to an exponential decay function using Kaleidograph. Half-lives measured from the curves are shown.

catalyzing splicing, degradation, and synthesis. In the expressions used, the concentration of the enzyme complex is implicit in the rate constants, with the exception of the equation for the rate of protein synthesis where the number of ribosomes that are actually translating the mRNA is explicit. The dilution of all compounds because of population growth was taken into account based on the specific growth rate μ of the cultures. Polyadenylation was not modeled as a separate process but implicitly included in the splicing equation. This yielded the following set of differential Equations 5–9,

$$\frac{d[\text{precursor}]}{dt} = v_{\text{transcription}} - (k_{\text{splicing}} + k_{\text{degrP}} + \mu) \times [\text{precursor}] \quad \text{(Eq. 5)}$$

$$\frac{d[PGKB\text{mRNA}]}{dt} = k_{\text{splicing}} \times [\text{precursor}] - (\mu + k_{\text{degrB}}) \times [PGKB\text{mRNA}] \quad \text{(Eq. 6)}$$

$$\frac{d[PGKC\text{mRNA}]}{dt} = k_{\text{splicing}} \times [\text{precursor}] - (\mu + k_{\text{degrC}}) \times [PGKC\text{mRNA}] \quad \text{(Eq. 7)}$$

$$\frac{d[PGKB\ \text{protein}]}{dt} = k_{\text{transl}} \times n_{\text{ribosome}} \times [PGKB\text{mRNA}] - (\mu + k_{\text{degrPGKB}}) \times [\text{PGKB protein}] \quad \text{(Eq. 8)}$$

$$\frac{d[\text{PGKC protein}]}{dt} = k_{\text{transl}} \times n_{\text{ribosome}} \times [PGKC\text{mRNA}] - (\mu + k_{\text{degrPGKC}}) \times [\text{PGKC protein}] \quad \text{(Eq. 9)}$$

The parameters used are described in Table 1, as are the values we used for them. The steady state of the system was calculated by setting all time derivatives equal to zero. The calculated steady-state magnitudes of the variables are given in the column marked Model A of Table 2. The steady state should be obtained experimentally when the trypanosomes have been in constant external conditions for a time much longer than the slowest relaxation time in the system. Here this should be a multiple of the inverse of the specific growth rate. The rate of transcription and the rate constant of translation were fitted to match the measured *PGKC* mRNA and PGKC protein, respectively, with that of the model. With the resulting parameter set also the model's *PGKB* mRNA concentration, which was not fitted, was close to the value determined experimentally. The calculated concentration of PGKB protein of slightly under 0.2 million per cell is probably an overestimate. We could not detect PGKB protein on Western blot without grossly over-

TABLE 1

Parameters characterizing PGK synthesis in bloodstream form T. brucei

To obtain the rate constants, half-lives reported in this study and elsewhere were recalculated to rate constants by using $k = \ln 2/t_{1/2}$, in which $t_{1/2}$ is the half-life in minutes and k the rate constant in min^{-1}.

Parameter	Value	Unit	Description	Origin of numbers
$v_{transcription}$	0.24	Molecules $cell^{-1}$ min^{-1}	Transcription rate	Fitted to match measured levels of *PGKC* mRNA
$k_{splicing}$	0.41	min^{-1}	Kinetic constant of splicing	This paper[a]
k_{degrP}	0.08	min^{-1}	Kinetic constant of precursor degradation	This paper
μ	0.0019	min^{-1}	Specific growth rate	Measured in cultures used in this study
k_{degrB}	0.092	min^{-1}	Kinetic constant of PGKB mRNA degradation	Observations with reporter constructs (34)
k_{degrC}	0.015	min^{-1}	Kinetic constant of PGKC mRNA degradation	Half- life of 45 min (33)
k_{transl}	13.4	Proteins $ribosome^{-1}$ min^{-1}	Kinetic constant of translation	Fitted to match measured levels of PGKC protein
*n*ribosome	12	Ribosomes $transcript^{-1}$	No. of ribosomes per transcript	This paper
$k_{degrPGKB}$	0	min^{-1}	Kinetic constant of PGKB degradation	This paper and as observed for other enzymes (11, 57, 82)
$k_{degrPGKC}$	0	min^{-1}	Kinetic constant of PGKC degradation	This paper and as observed for other genes (11, 57, 82)

[a] $k_{splicing} = k_{processing} - k_{degrP}$; $k_{processing}$ was measured by inhibition of transcription by actinomycin D (see also Fig. 2*C*).

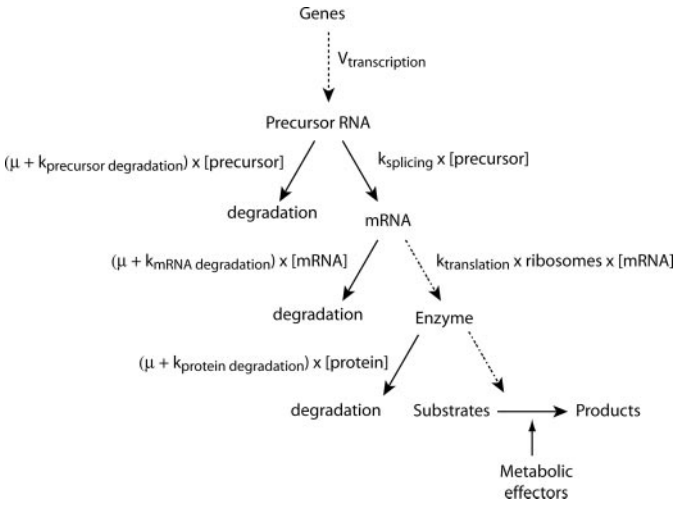

FIGURE 3. **General representation of factors affecting a metabolic process in trypanosomes.** Reactions used in our quantitative model for PGK expression are shown with rate equations. Parameters for these equations are described and listed in Table 1. Export of the mRNA from the nucleus is not included in the diagram. *Solid arrows* show mass flow; *dashed arrows* show an information flow. For brevity, *degradation* is written for degradation plus dilution because of population growth.

TABLE 2

Steady-state concentration of precursor and PGK mRNA and PGK protein in bloodstream form T. brucei (experimental data versus model values)

Model values in italics were the result of a fit to the experimental value and hence identical to that value.

	Measured	Model A	Model B	Units
Precursor	0.03 ± 0.01[a]	0.5	*0.05*	Molecules $cell^{-1}$
PGKB mRNA	0.8[a]	2	2.5	Molecules $cell^{-1}$
PGKC mRNA	12 ± 8	*12*	14	Molecules $cell^{-1}$
PGKB protein	ND[b]	1.8×10^5	2.1×10^5	Molecules $cell^{-1}$
PGKC protein	$1 \pm 0.5 \times 10^6$	*1×10^6*	1.2×10^6	Molecules $cell^{-1}$

[a] Bloodstream *T. brucei* have about 15× less PGKB mRNA than PGKC mRNA (33, 36).
[b] ND means not detectable.

loading the gel, and our detection limit was about 1×10^5 molecules per cell. This suggests that there is some negative translation regulation. This would make sense, because active PGKB protein in the cytosol would be detrimental to bloodstream form cells (31).

Based on the measured kinetics of precursor processing and RNA degradation, the model predicted that the precursor concentration would be 25 times lower than that of the mature *PGKC* mRNA, whereas a 300-fold lower concentration was measured (Table 2). According to the model the precursor RNA concentration is approximated by the transcription rate

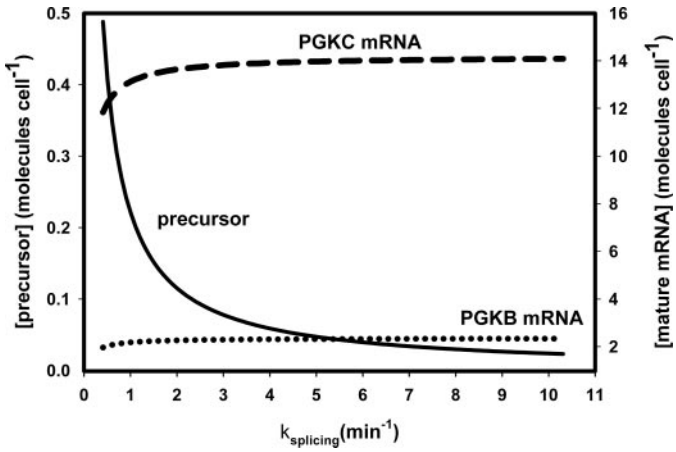

FIGURE 4. **Modeled relationship between $k_{splicing}$ and precursor and mRNA concentrations.**

divided by the splicing rate constant, given that the precursor degradation and dilution because of growth are slow compared with splicing (*cf.* Equation 5).

Given the technical limitations in our experiments, we considered the possibility that the actual splicing rate was faster than we had measured. A particular issue is that fact that actinomycin D may not have penetrated the cells instantaneously. Increasing $k_{splicing}$ in the model substantially lowered the concentration of the precursor with little effect on the mature messenger levels (Fig. 4). At a $k_{splicing}$ of 5 min^{-1}, the precursor level did correspond to the value determined experimentally. Decreasing the transcription rate in the model also decreased the precursor level. However, this also decreased the level of mature mRNAs to far below what was observed. This led us to formulate a model B which was identical to model A, except that the $k_{splicing}$ had been increased to 5 min^{-1}.

Control Analysis—Subsequently both models were used to calculate what controlled the concentrations of precursor RNA, PGKB mRNA, and PGKC mRNA in bloodstream forms, according to the concepts of metabolic control analysis. For model A this was done at the measured rate constant of splicing and for model B at the fitted splicing rate constant that led to the more realistic precursor concentration. We only show the results for model A in the main text, but we discuss how those of model B are different (see the Supplemental Material).

Transcription was fully limiting for the concentrations of all mRNAs, *i.e.* the corresponding control coefficients were all 1.00 (Table 3). In addition the steady-state concentrations of the two

TABLE 3
Concentration control coefficients calculated using Model A, i.e. $k_{splicing} = 0.41\ min^{-1}$, as was measured

Control on[a]	Control by							Sum[b]
	Transcription	Growth	Precursor degradation	Precursor splicing	Degradation *PGKB* mRNA	Degradation PGKC mRNA	Translation	
[Precursor]	1.00	0.00	−0.16	−0.83	0.00	0.00	0.00	0.00
[*PGKB* mRNA]	1.00	−0.02	−0.16	0.17	−0.98	0.00	0.00	0.00
[*PGKC* mRNA]	1.00	−0.12	−0.16	0.17	0.00	−0.89	0.00	0.00
[*PGKB* mRNA]/[*PGKC* mRNA]	0.00	0.09	0.00	0.00	−0.98	0.89	0.00	0.00
[PGKB protein]	1.00	−1.02	−0.16	0.17	−0.98	0.00	1.00	0.00
[PGKC protein]	1.00	−1.12	−0.16	0.17	0.00	−0.89	1.00	0.00
[PGKB protein]/[PGKC protein]	0.00	0.09	0.00	0.00	−0.98	0.89	0.00	0.00

[a] Brackets refer to number of molecules per cell.
[b] The sum was calculated before rounding off the numbers.

mature *PGK* mRNAs were controlled by processing of the precursor, by degradation of the mature and the precursor transcripts, and by cell growth. The control by the splicing process was positive, but control by all the others was negative, reflecting that activation of the latter three processes should *decrease* the mRNA concentrations (Table 3). In fact the control by mRNA degradation was almost as strong as that by transcription, and surprising to us with a much smaller control by the splicing process. Indeed, most of the negative control was exerted by degradation of the mature messengers.

The negative control by the growth process is something one could readily overlook in intuition-based analyses; mathematical calculations have the advantage that they tend to be comprehensive. This negative control is because of the halving of the number of mature mRNAs per cell at each cell division and can be particularly strong for the control of stable compounds in rapidly growing organisms. In our model the *PGKC* transcript concentration was more strongly controlled by the growth rate of the parasites than was the *PGKB* transcript concentration. By *in silico* experimentation with the model, we verified this difference was because the rate constant of *PGKB* mRNA degradation was 2 orders of magnitude higher than the specific growth rate, whereas that of *PGKC* mRNA degradation was closer to the specific growth rate. Somewhat more surprisingly, for both messengers the absolute control of mature transcript concentrations by the degradation of the precursor almost equaled that by the splicing (−0.16 and +0.17 respectively), whereas there is an 8-fold difference between their half-lives.

When the splicing rate constant $k_{splicing}$ was increased to 5 min^{-1} to match the measured precursor concentration (model B, see above), the control of precursor processing on the levels of mature messenger became even lower, *i.e.* −0.02 for control of precursor degradation and +0.02 for control of splicing on *PGKB* and *PGKC* mRNA levels. Most control was again exerted by transcription and mRNA degradation (see supplemental Table 3B).

In the model the control exerted by transcription, precursor degradation, precursor splicing, and mature mRNA degradation on the concentrations of the PGKB and PGKC protein concentrations equaled that exerted on the corresponding mRNA concentrations. This was because of the model assumption that translation and protein synthesis are unregulated and linearly dependent on the concentrations of mRNA and protein, respectively. This makes the steady-state protein concentrations linearly dependent on the corresponding steady-state mRNA concentrations (*cf.* Equations 8 and 9). However, not only transcription but also translation has strong positive control (1.00) on the level of PGK proteins. Because the sum of the concentration control coefficients should be zero again, there must be a negative contribution to compensate for this. Indeed the negative control coefficients by the growth rate are higher for the proteins than for the corresponding mRNAs, and the difference is precisely 1.00. In theory this extra negative control of −1.00 compared with the control of growth on mRNA levels could have resided in growth and protein degradation. However, because PGKC was shown to be stable in bloodstream forms, growth is the only factor that accounts for the extra negative control needed on the protein level.

In reality regulation of translation and/or protein degradation may modify the dependence of the protein concentrations on the mRNA concentrations, and this should then influence the control exerted by transcription and RNA processing on the protein concentrations. However, even in the latter case, the relative contributions of the processes at the RNA level to the control of protein concentrations should remain unaltered.

Regulation Analysis—To find out at which levels the cell regulates the mRNA levels when shifting from bloodstream form to procyclic form, we extended and applied regulation analysis (see Introduction). At steady state, the concentrations of each transcript *i* and of its precursor are constant (*cf.* Equations 5 and 6), see Equations 10 and 11,

$$\frac{d[mRNA_i]}{dt} = k_{splicing} \times [precursor] - (\mu + k_{degr\_i}) \times [mRNA_i] = 0 \quad \text{(Eq. 10)}$$

$$\frac{d[precursor]}{dt} = v_{transcription} - (k_{splicing} + k_{degrP} + \mu) \times [precursor] = 0 \quad \text{(Eq. 11)}$$

Combination of Equations 10 and 11 yields Equation 12,

$$[mRNA_i] = \frac{v_{transcription} \times k_{splicing}}{(k_{splicing} + k_{degrP} + \mu) \times (\mu + k_{degr\_i})} \quad \text{(Eq. 12)}$$

In logarithmic space we have Equation 13,

$$\log[mRNA_i] = \log v_{transcription} + \log\left(\frac{k_{splicing}}{k_{splicing} + k_{degrP} + \mu}\right) - \log(\mu + k_{degr\_i}) \quad \text{(Eq. 13)}$$

If we consider a transition from one state to another, *e.g.* from one life stage to the other, we have Equation 14,

$$\Delta\log[\mathrm{mRNA_i}] = \Delta\log\nu_{\mathrm{transcription}} + \Delta\log\left(\frac{k_{\mathrm{splicing}}}{k_{\mathrm{splicing}} + k_{\mathrm{degrP}} + \mu}\right) - \Delta\log(\mu + k_{\mathrm{degr\_}i}) \quad \text{(Eq. 14)}$$

Division through Δlog[mRNA] yields Equation 15,

$$1 = \rho_{\mathrm{transcription}} + \rho_{\mathrm{precursor\ processing}} + \rho_{\mathrm{degradation}} \quad \text{(Eq. 15)}$$

This can be written as Equation 16,

$$\frac{\Delta\log[\mathrm{mRNA_i}]}{\Delta\log[\mathrm{mRNA_i}]} = \frac{\Delta\log\nu_{\mathrm{transcription}}}{\Delta\log[\mathrm{mRNA_i}]} + \frac{\Delta\log\left(\frac{k_{\mathrm{splicing}}}{k_{\mathrm{splicing}} + k_{\mathrm{degrP}} + \mu}\right)}{\Delta\log[\mathrm{mRNA_i}]} - \frac{\Delta\log(\mu + k_{\mathrm{degr\_}i})}{\Delta\log[\mathrm{mRNA_i}]} \quad \text{(Eq. 16)}$$

Here the "transcription regulation coefficient of $\mathrm{mRNA_i}$," *i.e.* $\rho_{\mathrm{transcription}}$, quantifies the extent to which a specific steady-state mRNA concentration is regulated by the organism tuning the transcription of the corresponding gene. It equals $\Delta\log\nu_{\mathrm{transcription}}/\Delta\log\nu[\mathrm{mRNA_i}]$. $\rho_{precursor\ processing}$ quantifies the regulation of the steady-state mRNA concentration by the organism altering the precursor degradation and the splicing processes.

$$\rho_{precursor\ processing} = \frac{\Delta\log\frac{k_{\mathrm{splicing}}}{k_{\mathrm{splicing}} + k_{\mathrm{degrP}} + \mu}}{\Delta\log[\mathrm{mRNA_i}]} = \frac{\Delta\log\left(1 - \frac{k_{\mathrm{degrP}} + \mu}{k_{\mathrm{splicing}}}\right)}{\Delta\log[\mathrm{mRNA_i}]} \quad \text{(Eq. 17)}$$

$\rho_{\mathrm{degradation}}$ quantifies the regulation by the organism tuning the degradation of the processes and the mature mRNA or its growth rate. It equals minus $+ k_{\mathrm{degr\_}i})/\Delta\log[\mathrm{mRNA_i}]$.

It follows from these equations that regulation of mature mRNAs through changing precursor processing is negligible as long as *trans* splicing is fast compared with precursor degradation and cell growth. Then $k_{\mathrm{degrP}} + \mu \ll k_{\mathrm{splicing}}$ and $\rho_{\mathrm{precursor\ processing}}$ is very small. In particular, an increase in precursor processing could have no stronger effect than an increase in *PGKB* mRNA by 25% (which is also reflected in Fig. 4), whereas an ~23-fold increase is needed in the transition from bloodstream form to procyclics. Of course a very strong decrease in k_{splicing} could reduce the *PGKC* mRNA level, but to get 50% of the observed level in bloodstream forms, k_{splicing} should be lowered more than 85% (to 0.058 $\mathrm{min^{-1}}$) (see Fig. 4).

Although regulation of transcription of specific transcripts is believed to be absent in trypanosomes because of the polycistronic nature of transcription, $\rho_{\mathrm{transcription}}$ may still be substantial when the overall rate of transcription changes between two different conditions. From the known and measured changes in specific growth rate, mRNA degradation rates and mRNA concentrations, $\rho_{\mathrm{degradation}}$ was calculated. The sum $\rho_{\mathrm{transcription}} +$ $\rho_{\mathrm{precursor\ processing}}$ was then calculated from the summation theorem (Equation 15). Table 4 shows the results. The concentrations of *PGKB* and *PGKC* mRNA were predominantly regulated by their own degradation ($\rho_{\mathrm{degradation}}$ values of 0.85 and 0.84, respectively) and hardly by transcription or splicing. Because all values were prone to experimental errors, we calculated the effect of 2-fold changes in each individual degradation rate constant, and we found that mRNA degradation remained dominant in all cases. This is especially important in view of the uncertainty in the half-life of *PGKB* in procyclics (see above). A further increase of this half-life to 240 min did not substantially change the results; the $\rho_{\mathrm{degradation}}$ would become 1 and the contribution by transcription and splicing would be completely abolished.

TABLE 4

How T. brucei regulates PGK mRNA concentrations when it changes from its bloodstream form to its procyclic form

The degradation rate constants were calculated from the half-lives reported in the text, using the formula $k_{\mathrm{degr}} = \ln 2/t_{1/2}$; the mRNA concentrations were as reported in the text and Table 2. Concentrations are given in molecules/cell; μ (specific growth rate) and k_{degr} (degradation constant) values are in $\mathrm{min^{-1}}$.

	μ	*PGKB* mRNA		*PGKC* mRNA	
		Concentration	k_{degr}	Concentration	k_{degr}
Bloodstream form	0.0019	0.8	0.092	12	0.015
Procyclic form	0.0010	18	0.0058	1.0	0.14
$\rho_{\mathrm{degradation}}$		0.85		0.84	
$\rho_{\mathrm{transcription+splicing}}$		0.15		0.16	

DISCUSSION

In this study we report a comprehensive analysis of PGK gene expression in trypanosomes. The interesting issues are how the synthetic and coding capabilities of the organism are able to produce sufficient protein molecules, whether there are any bottlenecks, which processes control the overall process of mRNA and protein synthesis, and how the organism regulates expression levels when it undergoes the major switch from its bloodstream form to its procyclic form. Below we will discuss first our results in relation to previous results in the literature, and second their implications for our understanding of trypanosome gene expression.

Abundance of PGK mRNA and Protein—The number of *PGK* mRNA molecules per cell was quite low, and we wondered whether this was representative of mRNA more in general. We found that there were, on average, 12 *PGKC* and 72 *TUBA* mRNAs per cell. Among the 4632 expressed sequence tags (ESTs) from MVAT4 *T. brucei* rhodesiense bloodstream forms (61), we found 28 α-tubulin ESTs (0.6%) and 3 *PGK* ESTs (0.065%). For a total of 20,000 mRNAs per cell, the EST abundances would predict 121 *TUBA* and 13 *PGKC* mRNAs per cell. This suggests that representation in the EST data base is a reasonable indication of abundance. The EST frequencies for other glycolytic enzymes were between 1 and 4, suggesting that the mRNA abundances are likely to be similar to those of *PGKC*. For comparison, yeast cultivated in rich medium was estimated, by microarray analysis, to contain 60 *PGK* transcripts per cell. However, 80% of transcripts were present only at 0.1–2 molecules/cell (62). Estimates from solution hybridization for various mRNAs yielded estimates of <0.1–77 molecules per yeast cell (63).

TABLE 5
Statistics for bloodstream form trypanosome gene expression

Line	Model		*rRNA*	*VSG*	Total mRNA	*SLRNA*	*PGKC*	α-Tubulin
1	Mature transcript length (nucleotides)		6100	2710	2200	35	2140	1545
2	Transcript length (nucleotides)		8550[a]	2710[b]	2800[c]	140[c]	2340[c]	1745[c]
3	No. of genes/haploid genome[c]		4[d]	0.5	7400	75[d]	1	19[f]
4	No. of genes/average cell[g]		11.2	1.4	25,390	210	2.8	53
5	No. of molecules per cell[h]		125,000	1000[i]	20,000	20,000	12	72
6	Half-life		12 h[j]	45 min[j]	30 min[j]	30 min[j]	45 min[k]	30 min[l]
7	Transcript elongation rate nt/s[m]		40	40	20	20	20	20
8	Time to make one RNA (min)		3.6	1.2	2.25	0.12	2.0	1.4
9	Molecules $cell^{-1}$ h^{-1}	100% processing efficiency[n]	21,470	1038	3.0×10^4	3.0×10^4	12.5	108
10	RNAs per h per gene	100% processing efficiency[n]	1917	742	1.2	143	4.4	2.0
11	Distance between polymerases	100% processing efficiency[n]	75 bp	194 bp	61 kb	504 bp	16 kb	35 kb
12	Distance between polymerases	85% processing efficiency	64 bp	165 bp	52 kb	428 bp	14 kb	30 kb

[a] Primary transcript was deduced from genome sequence (83).
[b] Shown is *VSG117* mRNA.
[c] Data are from genome or EMBL database, and see "Experimental Procedures" and Supplemental Material.
[d] There are six annotated small subunit *rRNA* genes (83), but only four promoters as judged by Blast searching and four loci as judged by chromosome blotting (84).
[e] 100 gene copies per diploid genome by Southern blotting (85) and at least 60 by genome annotation (83).
[f] Data are from fiber-FISH hybridization (86).
[g] Data were calculated assuming 55% G_1, 30% S-phase, and 15% G_2/M (87) and on G_2 starting after 3.6 h (88).
[h] Measured values are from this paper, except for VSG.
[i] Data assume that 5% of mRNAs encoded VSG.
[j] From transcription inhibition experiments and the literature, see Supplemental Material for details. The value for total mRNA is based on half-lives varying from 12 min for actin to about 60 min for histone H4 (see Ref. 35 and A. Schwede, ZMBH, unpublished results).
[k] See Ref. 33.
[l] Data are from transcription inhibition experiments, see text.
[m] Assumed value was inserted into the calculations. The rate of yeast polymerase I has been estimated at 60 nt/s (69); results for mammalian cells are up to 95 nt/s (89, 90). The elongation rate for polymerase II is derived from measurements in yeast (91); for mammalian cells the average is about 30 nt/s, although if pausing is eliminated the rate is 70 bases/s (68).
[n] Data were calculated on a population basis, assuming continuous transcription and mRNA degradation and a constant ploidy of 2.8. 100% splicing efficiency, with a doubling of the RNA quantity once every cell cycle of 6 h, was also assumed. Values for 85% processing efficiency are in line 12.

According to our study a small number of mRNA molecules gave rise to approximately one million PGKC protein molecules per cell. The number of protein molecules per mRNA impressed us. We wondered whether this could be achieved with realistic translation rates. Our mathematical model enabled us to calculate the translation rate corresponding to these measurements. Assuming 12 ribosomes per mRNA, and 12 mRNAs per cell, it revealed that a translation rate of about 13 protein molecules per active ribosome per mRNA molecule/min should be needed (Table 1), and with a PGKC length of 440 amino acids this corresponds to 97 residues per active ribosome/s. The elongation rate for hen ovalbumin was estimated at 5 residues/s (64); in yeast at 30 °C with glucose, the average rate was 9 residues/s (65). Considering this, our calculation of the translation rate of PGK protein is rather high. Our ribosomal density estimate of up to 11–14 per mRNA seems reasonable; in a previous analysis of ribosome occupancy in yeast, the average number of ribosomes for a 2-kb mRNA was 10, and no RNA had more than 15 ribosomes, irrespective of length (66).

Cumulative errors in mRNA or protein estimates could provide an explanation for the high translation rate that we found. In multiple experiments we never found more than 20 *PGKC* mRNAs per trypanosome. Regarding protein, Misset *et al.* (67) determined that PGKC represented 0.16% of the total cellular protein in bloodstream form trypanosomes purified from rats. If 1 mg corresponds to 1.94×10^8 cells (17), this leads to an estimate of 1×10^5 molecules per cell, which should give a catalytic activity of 640 nmol min^{-1} mg cell $protein^{-1}$ (10). In the *in vitro* cultured trypanosomes that we use, PGK activity was 4.5-fold higher than this (11), whereas the protein estimate was 10-fold higher. Thus, our protein measurement is unlikely to be more than 2-fold too high. If, however, we assume 5×10^5 proteins per parasite, and 20 mRNAs, we arrive at a translation rate of 25 residues/s, which is only twice the yeast value. Because ribosomes could well elongate faster at 37 °C than at 30 °C, this does not seem unreasonable. The actual rate of translation does not influence the control analysis described in this paper, but it will result in a change in the steady-state concentration of PGKB and PGKC protein in the model predictions (Table 2).

The Rate of Transcription—We did not measure transcription rate directly in nuclear run-on experiments, because these are done on isolated nuclei and do not measure the *in vivo* rate. However, aided by the model we could calculate the rate of PGK transcription from our data (0.24 molecules per cell per min). Table 5 shows the results of a more detailed analysis, as further described in the Supplemental Material. The inter-polymerase spacings for both RNA polymerase I and RNA polymerase II genes that we calculated were based on the number of mRNAs that have to made in a certain amount of time, and they were consistent with values previously reported for other eukaryotes (63, 69–72). Given the rate of RNA polymerases and the number of genes to be transcribed, the required average RNA polymerase II spacing of around 50 kb on protein-coding genes means that at any given time, as in other eukaryotes (73, 74), many open reading frames are not being transcribed. As expected, the RNA polymerase I density for variant surface glycoprotein and *rRNA* loci was predicted to be much higher than 1/50 kb. For *PGKC* and *TUBA*, the average polymerase spacings were predicted to be 14 and 30 kb, respectively, in bloodstream forms.

The Kinetics of Splicing—When we treated trypanosomes with actinomycin D, the precursor mRNA was spliced with a half-life of about 1 min. This result is similar to earlier observa-

tions of permeabilized procyclic trypanosomes, showing *trans* splicing of α-tubulin, β-tubulin, and actin pre-mRNAs within 1–2 min of synthesis of the 3′ splice site (75). Because actinomycin D also inhibits *SLRNA* synthesis, it could potentially interfere with splicing. However, this is probably not significant in our experiments because (in procyclic forms) the *SLRNA* has a half-life of 8 min (76). If the measured half-time for splicing is typical, RNAs will be spliced when polymerase II has progressed 1200 nt downstream, based on a polymerase II rate of 20 nucleotides/s (Table 5). Yeast mRNAs also are spliced within 1 min of formation of the 3′ splice site (77–79), and selected mammalian introns had half-lives ranging from 0.4 to 7.5 min (80). The similarity of trypanosome *trans* splicing kinetics with those for *cis* splicing in other organisms is quite surprising given that *trans* splicing is a two-substrate reaction. Therefore, first-order decay of the precursor pool suggests that in *T. brucei*, the steady-state *SLRNA* pool is high enough to remain saturating throughout the experiment. Interestingly, this may not be true for all kinetoplastids; the steady-state level of *SLRNA* varies over a 4-fold range in different *Leishmania* species, and an increase in the number of *SLRNA* genes in *Leishmania major* resulted in an increase in virulence (81).

Transcription and Trans Splicing Does Not Regulate Mature PGK mRNA Levels—A central question of this study was how mRNA concentrations were regulated in trypanosomes. It was known already that changes in the mRNA degradation pathway can have a major effect on mRNA levels. For instance, depletion of the exonuclease XRNA increased the stability of *PGKB* mRNA in bloodstream forms, with a concomitant increase in mRNA abundance. It also increased the *PGKC* mRNA half-life and level in procyclics, consistent with a major control by mRNA degradation (35). However, these results do not necessarily imply that the cell uses degradation to regulate mRNA levels. This study now quantitatively shows that the cells do use messenger degradation for regulation and that regulation of other processes makes a very minor contribution, and we will summarize and discuss the basis for this conclusion.

In metabolic control analysis concentration control coefficients always sum up to zero (5). In the particular example studied here, this implied that the negative control exerted by mRNA degradation on mRNA concentrations was balanced by a positive control exerted at the mRNA production side. This could then have been splicing or transcription. Our model calculations showed that in reality the lions share of the positive control was in transcription, with very little positive control in splicing. This means that there is a potential to regulate mRNA levels via transcription; if the transcription rate were to change, this should strongly affect the concentrations of the mature mRNA.

The derivation of the regulation coefficients showed that even in trypanosomes transcription could contribute to the regulation of mRNA concentrations, for example if the overall transcription rate were to differ between procyclic and bloodstream forms (see Equations 15 and 16). This somewhat counterintuitive result is because of the fact that we considered the absolute concentrations of mRNAs rather than their concentrations relative to each other. When we considered the control of the ratio of the two mRNAs (see Table 3), we found that that this ratio was not controlled by transcription but was virtually only controlled by the specific degradation processes of the two mRNAs. Indeed it follows from Equation 12 that all mRNAs that are derived from the same precursor are equally sensitive to changes in the transcription rate, implying that the transcription rate cannot regulate their relative concentrations.

The fact that transcription strongly controlled the PGK mRNA concentrations in exponentially growing bloodstream form trypanosomes could suggest that the organism also used this to regulate its mRNA concentrations when it transforms to the procyclic form. We found that this is not the case at all; the regulation coefficients of absolute concentrations of *PGKB* and *PGKC* mRNA by transcription and precursor processing together were close to zero, demonstrating that the absolute mRNA concentrations were hardly regulated by these processes. These results illustrate the difference between control and regulation coefficients; even though the *control* exerted by transcription was high, it did not *regulate* the mRNA levels.

The second striking result that we obtained was that the regulation by splicing was negligible. Previously, two groups have investigated trypanosome splicing efficiency by measuring the expression of luciferase protein from reporter genes with different 5′-untranslated regions (5′-UTRs) and splicing signals. There were several differences in reporter protein expression depending on the sequences used, but the groups came to diametrically opposite conclusions (37, 38). One group, which changed the splicing signal but not the 5′-UTR, concluded that the *PGKC* signal functioned poorly in procyclic trypanosomes (38). The other group used splicing signals with the 5′-UTR and found no difference between the *PGKB* and *PGKC* signals (37). Here we used a different type of analysis. We did not just ask the question whether sequence differences could give rise to different splicing efficiencies, but to what extent changes of the splicing rate constant could have affected (control) and were varied to affect (regulation) the mature mRNA concentrations during differentiation.

The regulation coefficients that we obtained were consistent with a predominant regulation by mRNA degradation, without any substantial contribution by precursor processing. Even though the experimental data, from which the regulation coefficients were calculated, were highly error-prone, we checked that a 2-fold uncertainty in the mRNA half-lives changed the regulation coefficients only marginally.

The most convincing argument, however, against a role for *trans* splicing in the regulation of mature *PGK* mRNA concentration is that the potential to regulate is limited. This is seen from the control coefficients as well as from the response to larger changes in splicing rate constant. The control coefficients by splicing were very small (0.17 only), requiring phenomenal changes in splicing activity for a strong change in mRNA abundance to result. Moreover, the mature mRNA concentrations depended hyperbolically on the splicing rate constant (Equation 13). In the bloodstream trypanosomes, the splicing rate constant was close to saturating, and no increase in the splicing activity could increase the level of mature mRNA by more than 25% (Fig. 4). The basis for this is that transcription is an irreversible process. and whether spliced rapidly or not, the precursor will end up as mature mRNA. The only processes

detracting from this are as follows: (i) growth, *i.e.* if growth were rapid enough then splicing rates might not be fast enough to supply daughter cells with sufficient mature mRNA, or (ii) precursor degradation. However, precursor degradation was five times slower than splicing and could therefore not have much effect, and growth was even 2 orders of magnitude slower than splicing. Even though the precise rate constants are difficult to determine, the difference between splicing and precursor degradation kinetics was quite convincing (Fig. 2), which corroborates our conclusion that the splicing rate constant hardly controlled the mature mRNA concentrations in this case. A further decrease of the splicing rate constant, however, would start to affect the mature mRNA concentrations, demonstrating that in the case of the *PGK* genes splicing was only just fast enough compared with precursor degradation to lose control (Fig. 4). The interplay between splicing and precursor degradation also becomes apparent in the fact that their (small) concentration control coefficients were virtually equal but of opposite sign (Table 3), demonstrating that the *potential* to regulate mRNA concentrations via precursor degradation is as high as via splicing.

In the above analysis it is assumed that splicing and precursor degradation compete. however, it could be that precursors are only degraded if splicing is inhibited, in which case precursor degradation would be irrelevant in healthy exponentially growing cells. In the latter case the rate constant for precursor degradation becomes zero, and changes in the splicing rate constant do not affect mRNA pools at all (Equation 13). When the 5′-3′-exonuclease XRNA (which is in both nucleus and cytoplasm) was depleted in bloodstream trypanosomes, the results obtained were consistent with a role for XRNA in precursor degradation, and with competition between precursor degradation and splicing (35).

We emphasize that the control analysis was only carried out in the bloodstream form. It is conceivable that the distribution of control shifts during differentiation to the insect form. Furthermore, our study was limited to the *PGK* genes, and it remains to be seen how other mRNAs are controlled and regulated. However, the conclusion that splicing can only regulate mRNA concentrations if it is slow compared with precursor degradation is general and holds for all mRNAs. Finally, this study yields a theoretical framework, which can be used to dissect regulation of other genes and in other organisms, including organisms in which transcription is regulated.

Acknowledgments—We thank Claudia Hartmann, Chi-Ho Li, and Dirk Bald for help with methods and Paul Michels for insightful discussions. The E. coli TbPGKC expression system and the antibody Do425 were kind gifts of Prof. Paul Michels.

REFERENCES

1. Kacser, H., and Burns, J. A. (1973) *Symp. Soc. Exp. Biol.* **27,** 65–104
2. Heinrich, R., and Rapoport, T. A. (1974) *Eur. J. Biochem.* **42,** 89–95
3. Westerhoff, H. V., Koster, J. G., Van Workum, J. G., and Rudd, K. E. (1990) in *Control of Metabolic Processes* (Cornish-Bowden, A., and Cardenas, M. L., eds) pp. 399–412, Plenum Publishing Corp., New York
4. Heinrich, R., and Schuster, S. (1996) *The Regulation of Cellular Systems*, Chapman & Hall, New York
5. Westerhoff, H. V., and Van Dam, K. (1987) *Thermodynamics and Control of Biological Free Energy Transduction*, Elsevier Science Publishers B.V., Amsterdam
6. Kahn, D., and Westerhoff, H. V. (1991) *J. Theor. Biol.* **153,** 255–285
7. Hornberg, J. J., Bruggeman, F. J., Binder, B., Geest, C. R., de Vaate, A. J., Lankelma, J., Heinrich, R., and Westerhoff, H. V. (2005) *FEBS J.* **272,** 244–258
8. Snoep, J. L., van der Weijden, C. C., Andersen, H. W., Westerhoff, H. V., and Jensen, P. R. (2002) *Eur. J. Biochem.* **269,** 1662–1669
9. Teusink, B., Passarge, J., Reijenga, C., Esgalhado, E., van der Weijden, C., Schepper, M., Walsh, M., Bakker, B., van Dam, K., Westerhoff, H., and Snoep, J. (2000) *Eur. J. Biochem.* **267,** 5313–5329
10. Bakker, B. M., Michels, P. A. M., Opperdoes, F. R., and Westerhoff, H. V. (1997) *J. Biol. Chem.* **272,** 3207–3215
11. Albert, M.-A., Haanstra, J., Hannaert, V., Van Roy, J., Opperdoes, F., Bakker, B., and Michels, P. (2005) *J. Biol. Chem.* **280,** 28306–28315
12. ter Kuile, B., and Westerhoff, H. (2001) *FEBS Lett.* **500** 169–171
13. Rossell, S., van der Weijden, C., Kruckeberg, A., Bakker, B., and Westerhoff, H. (2005) *FEMS Yeast Res.* **5,** 611–619
14. Daran-Lapujade, P., Rossell, S., van Gulik, W. M., Luttik, M. A., de Groot, M. J., Slijper, M., Heck, A. J., Daran, J. M., de Winde, J. H., Westerhoff, H. V., Pronk, J. T., and Bakker, B. M. (2007) *Proc. Natl. Acad. Sci. U. S. A.* **104,** 15753–15758
15. Bruggeman, F., and Westerhoff, H. (2007) *Trends Microbiol.* **15,** 45–50
16. van Weelden, S. W., van Hellemond, J. J., Opperdoes, F. R., and Tielens, A. G. (2005) *J. Biol. Chem.* **280,** 12451–12460
17. Bakker, B. M., Walsh, M. C., ter Kuile, B. H., Mensonides, F. I. C., Michels, P. A. M., Opperdoes, F. R., and Westerhoff, H. V. (1999) *Proc. Natl. Acad. Sci. U. S. A.* **96,** 10098–10103
18. Michels, P. A. M., Hannaert, V., and Bringaud, F. (2000) *Parasitol. Today* **16,** 482–489
19. Helfert, S., Estévez, A., Bakker, B., Michels, P., and Clayton, C. E. (2001) *Biochem. J.* **357,** 55–61
20. Furuya, T., Kessler, P., Jardim, A., Schnaufer, A., Crudder, C., and Parsons, M. (2002) *Proc. Natl. Acad. Sci. U. S. A.* **99,** 14177–14182
21. Kessler, P. S., and Parsons, M. (2005) *J. Biol. Chem.* **280,** 9030–9036
22. Martinez-Calvillo, S., Nguyen, D., Stuart, K., and Myler, P. J. (2004) *Eukaryot. Cell* **3,** 506–517
23. Martinez-Calvillo, S., Yan, S., Nguyen, D., Fox, M., Stuart, K., and Myler, P. J. (2003) *Mol. Cell* **11,** 1291–1299
24. McAndrew, M., Graham, S., Hartmann, C., and Clayton, C. E. (1998) *Exp. Parasitol.* **90,** 65–76
25. Liang, X., Haritan, A., Uliel, S., and Michaeli, S. (2003) *Eukaryot. Cell* **2,** 830–840
26. Clayton, C. E. (2002) *EMBO J.* **21,** 1881–1888
27. Gibson, W. C., Swinkels, B. W., and Borst, P. (1988) *J. Mol. Biol.* **201,** 315–325
28. Alexander, K., and Parsons, M. (1991) *Mol. Biochem. Parasitol.* **46,** 1–10
29. Alexander, K., and Parsons, M. (1993) *Mol. Biochem. Parasitol.* **60,** 265–272
30. Misset, O., and Opperdoes, F. R. (1987) *Eur. J. Biochem.* **162,** 493–500
31. Blattner, J., Helfert, S., Michels, P., and Clayton, C. E. (1998) *Proc. Natl. Acad. Sci. U. S. A.* **95,** 11596–11600
32. Blattner, J., and Clayton, C. E. (1995) *Gene* (*Amst.*) **162,** 153–156
33. Colasante, C., Robles, A., Li, C.-H., Schwede, A., Benz, C., Voncken, F., Guilbride, D. L., and Clayton, C. (2007) *Mol. Biochem. Parasitol.* **151,** 193–204
34. Haile, S., Estévez, A. M., and Clayton, C. (2003) *RNA* (*N. Y.*) **9,** 1491–1501
35. Li, C.-H., Irmer, H., Gudjonsdottir-Planck, D., Freese, S., Salm, H., Haile, S., Estévez, A. M., and Clayton, C. E. (2006) *RNA* (*N. Y.*) **12,** 2171–2186
36. Quijada, L., Hartmann, C., Guerra-Giraldez, C., Drozdz, M., Irmer, H., and Clayton, C. E. (2002) *Nucleic Acids Res.* **30,** 1–11
37. Kapotas, N., and Bellofatto, V. (1993) *Nucleic Acids Res.* **21,** 4067–4072
38. Siegel, T., Tan, K., and Cross, G. (2005) *Mol. Cell. Biol.* **25,** 9586–9594
39. Parsons, M., and Hill, T. (1989) *Mol. Biochem. Parasitol.* **33,** 215–228
40. Biebinger, S., Wirtz, L. E., and Clayton, C. E. (1997) *Mol. Biochem. Parasitol.* **85,** 99–112
41. van Deursen, F. J., Shahi, S. H., Turner, C. M. R., Hartmann, C., Guerra-

Giraldez, C., Matthews, K. R., and Clayton, C. E. (2001) *Mol. Biochem. Parasitol.* **112,** 163–172
42. Dovey, H. F., Parsons, M., and Wang, C. C. (1988) *Proc. Natl. Acad. Sci. U. S. A.* **85,** 2598–2602
43. Liu, L., Liang, X., Uliel, S., Unger, R., Ullu, E., and Michaeli, S. (2002) *J. Biol. Chem.* **277,** 47348–47357
44. Mandelboim, M., Barth, S., Biton, M., Liang, X., and Michaeli, S. (2003) *J. Biol. Chem.* **278,** 51469–51478
45. Hendriks, E. F., Abdul-Razak, A., and Matthews, K. R. (2003) *J. Biol. Chem.* **278,** 26870–26878
46. Djikeng, A., Shi, H., Tschudi, C., Shen, S., and Ullu, E. (2003) *RNA* (*N. Y.*) **9,** 802–808
47. Zomer, A. W., Allert, S., Chevalier, N., Callens, M., Opperdoes, F. R., and Michels, P. A. (1998) *Biochim. Biophys. Acta* **1386,** 179–188
48. Schilling, M., Maiwald, T., Bohl, S., Kollmann, M., Kreutz, C., Timmer, J., and Klingmuller, U. (2005) *FEBS J.* **272,** 6400–6411
49. Sauro, H. M. (2000) in *Animating the Cellular Map: Proceedings of the 9th International Meeting on BioThermoKinetics* Stellenbosch, April 3–8, 2000, (Hofmeyr, J. H. S., Rohwer, J. M., and Snoep, J. L., eds) Stellenbosch University Press, South Africa
50. Sauro, H. M., Hucka, M., Finney, A., Wellock, C., Bolouri, H., Doyle, J., and Kitano, H. (2003) *OMICS* **7,** 355–372
51. Pays, E., Hanocq-Quertier, J., Hanocq, F., Van Assel, S., Nolan, D., and Rolin, S. (1993) *Mol. Biochem. Parasitol.* **61,** 107–114
52. Waldron, C., and Lacroute, F. (1975) *J. Bacteriol.* **122,** 855–865
53. Clayton, C. E. (1985) *EMBO J.* **4,** 2997–3003
54. Mottram, J., Murphy, W., and Agabian, N. (1989) *Mol. Biochem. Parasitol.* **37,** 115–127
55. Pays, E., Delronche, M., Lheureux, M., Vervoort, T., Bloch, J., Gannon, F., and Steinert, M. (1980) *Nucleic Acids Res.* **8,** 5965–5981
56. Allen, T. E., and Ullman, B. (1993) *Nucleic Acids Res.* **21,** 5431–5438
57. Clayton, C. E. (1988) *Mol. Biochem. Parasitol.* **28,** 43–46
58. Sobell, H. M. (1985) *Proc. Natl. Acad. Sci. U. S. A.* **82,** 5328–5331
59. McNally, K. P., and Agabian, N. (1992) *Mol. Cell. Biol.* **12,** 4844–4851
60. Ullu, E., and Tschudi, C. (1991) *Proc. Natl. Acad. Sci. U. S. A.* **88,** 10074–10078
61. Djikeng, A., Agufa, C., Donelson, J. E., and Majiwa, P. A. (1998) *Gene* (*Amst.*) **221,** 93–106
62. Holstege, F., Jennings, E., Wyrick, J., Lee, T., Hengartner, C., Green, M., Golub, T., Lander, E., and Young, R. (1998) *Cell* **95,** 717–728
63. Iyer, V., and Struhl, K. (1996) *Proc. Natl. Acad. Sci. U. S. A.* **93,** 5208–5212
64. Palmiter, R. (1975) *Cell* **4,** 189–197
65. Bonven, B., and Gullov, K. (1979) *Mol. Gen. Genet.* **170,** 225–230
66. Arava, Y., Wang, Y., Storey, J., Liu, C., Brown, P., and Herschlag, D. (2003) *Proc. Natl. Acad. Sci. U. S. A.* **100,** 3889–3894
67. Misset, O., Bos, O. J. M., and Opperdoes, F. R. (1986) *Eur. J. Biochem.* **157,** 441–453
68. Darzacq, X., Shav-Tal, Y., de Turris, V., Brody, Y., Shenoy, S. M., Phair, R. D., and Singer, R. H. (2007) *Nat. Struct. Mol. Biol.* **14,** 796–806
69. French, S., Osheim, Y., Cioci, F., Nomura, M., and Beyer, A. (2003) *Mol. Cell. Biol.* **23,** 1558–1568
70. Kettenberger, H., Armache, K., and Cramer, P. (2004) *Mol. Cell* **16,** 955–965
71. Chubb, J., Trcek, T., Shenoy, S., and Singer, R. (2006) *Curr. Biol.* **16,** 1018–1025
72. Bon, M., McGowan, S., and Cook, P. (2006) *FASEB J.* **20,** E1071–E1074
73. Kimura, H., Sugaya, K., and Cook, P. R. (2002) *J. Cell Biol.* **159,** 777–782
74. Jackson, D. A., Pombo, A., and Iborra, F. J. (2000) *FASEB J.* **14,** 242–254
75. Ullu, E., Matthews, K. R., and Tschudi, C. (1993) *Mol. Cell. Biol.* **13,** 720–725
76. Biton, M., Mandelboim, M., Arvatz, G., and Michaeli, S. (2006) *Mol. Biochem. Parasitol.* **150,** 132–143
77. Lacadie, S. A., and Rosbash, M. (2005) *Mol. Cell* **19,** 65–75
78. Tardiff, D., Lacadie, S., and Rosbash, M. (2006) *Mol. Cell* **24,** 917–929
79. Gornemann, J., Kotovic, K. M., Hujer, K., and Neugebauer, K. M. (2005) *Mol. Cell* **19,** 53–63
80. Audibert, A., Weil, D., and Dautry, F. (2002) *Mol. Cell. Biol.* **22,** 6706–6718
81. Zhang, W.-W., and Matlashewski, G. (2004) *Mol. Microbiol.* **54,** 1051–1062
82. Clayton, C. E. (1987) *J. Cell Biol.* **105,** 2649–2653
83. Berriman, M., Ghedin, E., Hertz-Fowler, C., Blandin, G., Renauld, H., Bartholomev, D. C., Lennard, N. J., Caler, E., Hamlin, N. E., Haas, B., Böhme, U., Hannick, L., Aslett, M. A., Shallom, J., Marcello, L., *et al.* (2005) *Science* **309,** 416–422
84. Zomerdijk, J., Kieft, R., and Borst, P. (1992) *Nucleic Acids Res.* **20,** 2725–2734
85. de Lange, T., Liu, A., Van der Ploeg, L., Borst, P., Tromp, M., and Van Boom, J. (1983) *Cell* **34,** 891–900
86. Ersfeld, K., Asbeck, K., and Gull, K. (1998) *Chromosoma* **107,** 237–240
87. Tu, X., and Wang, C. C. (2005) *Eukaryot. Cell* **4,** 755–764
88. McKean, P. G. (2003) *Curr. Opin. Microbiol.* **6,** 600–607
89. Dundr, M., Hoffmann-Rohrer, U., Hu, Q., Grummt, I., Rothblum, L., Phair, R., and Misteli, T. (2002) *Science* **298,** 1623–1626
90. Grummt, I. (2003) *Genes Dev.* **17,** 1691–1702
91. Bentley, D. (2005) *Curr. Opin. Cell Biol.* **17,** 251–256